A Theory of Time-Reversed Impulse Multiple-Input Multiple-Output (MIMO) for Ultra-Wideband (UWB) Communications

(Invited Paper)

Robert C. Qiu
Department of Electrical and Computer Engineering
Center for Manufacturing Research
Tennessee Technological University
Cookeville, TN 338505
Email: rqiu@tntech.edu

***Abstract*— This paper proposes a new approach to taking advantage of rich multipath through the use of time-reversal combined with impulsive Multiple-Input Multiple-Output (MIMO) for Ultra-Wideband (UWB) Communications. A comprehensive review of literature is also given.**

I. Introduction

Ultra-wide bandwidth (UWB) communications has been studied in the pioneering work of Win and Scholtz [7]-[8]. The first UWB propagation measurements are reported in the literature [9]- [13]. Narrowband interference effect is considered in [14], and a complete spectral analysis is carried out in [15] [16]. Acquisition of UWB signals is critical, and its fundamental limits are given in [18] [19].

The most pressing and challenging problem, caused by the unprecedented bandwidth, may be the increased transceiver complexity [20]. The impulsive UWB pulses [21]-[24] require extremely high sampling rates as well as accurate timing synchronization. As a result, such coherent transceivers as RAKE and Orthogonal Frequency Division Multiplexing (OFDM), used in IEEE 802.15.3a, are too complicated for current application. Capture of energy from such a large number of weak paths is challenging to RAKE based solutions. Processing many wideband carriers in OFDM is complex, as well. For these reasons, a transmitted reference based transceiver has been proposed [17] [56] [59] [64], but requires a long delay line that is very difficult to be implemented in hardware. As a result, UWB community is forced to use noncoherent receivers like energy detection in IEEE 802.15.4a for sensors and RFID applications. This type of receiver can be implemented, using such cheap analog components as schottky, tunnel and germanimum diodes, for its detector.

The momentum of UWB technology is mainly thwarted by the practical aspects. Our vision is that impulse radio is a next-generation technology of great potential. The low-complexity, energy-detecting receiver provides the first commercially feasible solution to a broad class of low-data-rate applications such as IEEE 802.15.4a. The challenge of high-data-rate solutions facing OFDM and RAKE, however, remains unresolved. Is it possible to follow the path of IEEE 802.15.4a to use low-cost receivers for high data rates? The transceiver complexity and thus its cost are, after all, the dominant factors that limit these high-data-rate commercial applications. The current solutions in the literature cannot provide a satisfying answer to this need. The IEEE 802.15.3a working group was just disbanded in 2006, leaving RAKE and OFDM based technologies to compete in the marketplace. The main driver for this disbanding has been the different views of how to reduce the transceiver complexity. One wonders whether there is a better alternative to the two unsatisfying system paradigms.

The proposed system paradigm uses time-reversal with noncoherent detection as an alternative to coherent reception. It exploits the hostile, rich-multipath channel as part of the receiver chain. This new method also combines time-reversal with MIMO, the most promising approach to use spectrum and transmission power. As a result, time-reversal trades the huge bandwidth of UWB radio and the high power efficiency of MIMO for the noncoherent detection of extremely low cost. This proposed new system paradigm is to take advantage of the impulse nature of UWB signals, a new dimension of a communication channel, through time-reversed MIMO. The new dimension of impulsive time-reversal adds more degrees of freedom in exploiting the spatiotemporal dimensions.

A. Time-Reversal—A Review

Time-reversal in acoustics [25-38] is closely related to retrodirective array in microwave [39]-[41] and phase-conjugation in optics. Time-reversal is used in UWB recently [42]-[61]. The original motivation of time-reversal is to use the ocean as correlator in saving calculation of correlation, limited by the computing capabilities of 1960s. Time-reversal mirror is a generalization of an optical phase-conjugated mirror in the sense that the time-reversal mirror applies to pulsed broadband signals [26][27], rather than to monochromatic ones.

Another use of time-reversal is related with compensation for distortions, caused by multipath and unknown antenna array deformation, which limit the capacity of underwater communications [31]-[38]. Furthermore, time-reversal can confine acoustic energy to a narrow beam that will track the intended receiver [31], called spatial focusing. In 1990s shallow-water acoustic communications systems are forced to rely on noncoherent processing techniques because of complexity in the acoustic environment [31]. This is true for the state-of-the-art of UWB communications today. *Time-reversal* was explored [32] to be an *alternative to coherent underwater communications*. The first experimental demonstration of time-reversal was done in [34]. Time-reversal is regarded as an environmentally self-adaptive process in complicated ocean environments. The primary result is that the time-reversal mirror focus is robust. Rather simple signal processing is used. A new method of using time-reversal for coherent communication was experimentally demonstrated [28]. The first known application of *non-coherent time-reversal* was experimentally demonstrated [36,37], using a *non-coherent envelope detector* at the expense of increased complexity in the transmitter.

Time-reversal is used for electromagnetic waves [40] [41]. The use of time-reversal in UWB wireless communications is relatively new [42]- [61]. The combination of time-reversal with UWB-MIMO does not appear in the literature. Pre-coding using time-division duplexing and pre-RAKE are related to time-reversal. Time-reversal does not use the capacity-achieving power allocation. Time-reversal is used in [61] to compensate for per-path pulse distortion [60]- [67].

II. Time-Reversed Impulse MIMO

A. System Framework

Let us consider the system block diagram of the time-reversed impulse MIMO in Fig. 1. Energy-detection is used. The following derivation in the time domain is in parallel with that of [30] in the frequency domain. Let us denote $h_{mn}(t)$ the channel impulse response (CIR) relating the m-th element at the transmitter to the n-th element at the receiver. The set of impulse responses is called the propagation operator. If one sends pulsed signal $a_m(t), m = 1, ..., M$ from the transmit array, the signal $b_n(t)$ is obtained in the receive array as

$$b_n(t) = \sum_{m=1}^{M} h_{nm}(t) * a_m(t), n = 1, ..., N \quad (1)$$

Or, in matrix form,

$$\mathbf{b(t)} = \mathbf{H(t)} * \mathbf{a(t)} \quad (2)$$

where $\mathbf{b(t)} = [\mathbf{b_1(t)}, \mathbf{b_2(t)}, ..., \mathbf{b_N(t)}]^{\dagger}$, $\mathbf{a(t)} = [\mathbf{a_1(t)}, \mathbf{a_2(t)}, ..., \mathbf{a_M(t)}]^{\dagger}$, and $\mathbf{H(t)}$ is the matrix of $N \times M$ with elements of $h_{nm}(t)$. The notation of "$*$" represents element-by-element convolution; the superscript "$\dagger$" represents the conjugate transpose (Hermitian) of a vector or matrix. On the other hand, due to the spatial reciprocity, if one sends a signal $c_m, m = 1, ..., M$ from the receive array, the signal $d_n(t), n = 1, ..., N$ is obtained in the transmit array. Defining column vectors $\mathbf{c}$ and $\mathbf{d}$ as $\mathbf{a}$ and $\mathbf{b}$, respectively, it follows that

$$\mathbf{d(t)} = \mathbf{H}^{\dagger}\mathbf{(t)} * \mathbf{c(t)} \quad (3)$$

As a consequence, $\mathbf{H(t)}$ permits one to calculate the forward propagation of impulses from the transmit array to the receive array, while $\mathbf{H}^{\dagger}\mathbf{(t)}$ the backward propagation from the receive array to the transmit array.

A time-reversal focusing is a two-step process: (1) first backward propagation and (2) then forward propagation. The two steps can be regarded as the combination of the backward propagation process described by Eq. (2) with the forward propagation process described by Eq. (3). The time-reversal process begins by sending the $N \times 1$ vector $\mathbf{p(t)} = [\mathbf{p_1(t)}, ..., \mathbf{p_N(t)}]^{\dagger}$ from the receive array, where $p_n(t)$ is the pulse waveform emitted from the n-th antenna. Then the signal obtained at the transmit array after the backward propagation is expressed according to Eq. (3) as the $M \times 1$ vector $\mathbf{g(t)} = [\mathbf{g_1(t)}, ..., \mathbf{g_M(t)}]^{\dagger}$ given by

$$\mathbf{g(t)} = \mathbf{H}^{\dagger}\mathbf{(t)} * \mathbf{p(t)} \quad (4)$$

where $g_n(t)$ is the pulse waveform obtained at the m-th antenna of the transmit array. In the second step, the recorded signal at the transmit array $\mathbf{g(t)}$ is time-reversed to yield

$$\mathbf{g(-t)} = \mathbf{H}^{\dagger}\mathbf{(-t)} * \mathbf{p(-t)} \quad (5)$$

The time-reversed signals $g_n(-t)$, $n = 1, 2, ..., N$, are modulated with information-bearing pulsed waveforms $x_{km}(t)$, $k = 1, 2, ..., N$, $m = 1, 2, ..., M$, and the resultant M pulsed waveforms corresponding to N antennas at the transmit array are given by

$$q_m(t) = \sum_{k=1}^{M} x_{mk}(t) * g_k(-t), m = 1, ..., M \quad (6)$$

Or, in matrix form,

$$\mathbf{q(t)} = \mathbf{X(t)} * \mathbf{g(-t)} = \mathbf{X(t)} * \mathbf{H}^{\dagger}\mathbf{(-t)} * \mathbf{p(-t)} \quad (7)$$

where $\mathbf{q(t)} = [\mathbf{q_1(t)}, ..., \mathbf{q_M(t)}]^{\dagger}$ is an $N \times 1$ vector, and the mk-th element of the $M \times M$ matrix $\mathbf{X(t)}$ is $x_{mk}(t)$[1]. The resultant modulated signal collected in the vector $\mathbf{q(t)}$ is again re-transmitted from the transmit array. By combining Eq. (2), Eq. (5) and Eq. (7), the signal $\mathbf{y(t)}$ obtained at the receive array is expressed as

$$\mathbf{y(t)} = \mathbf{H(t)} * \mathbf{X(t)} * \mathbf{H}^{\dagger}\mathbf{(-t)} * \mathbf{p(-t)} \quad (8)$$

where the $N \times 1$ vector $\mathbf{y(t)}$ has its n-th element $y_n(t)$ corresponding to the n-th antenna. $\mathbf{y(t)}$ is the signal obtained in the receive array after time-reversal re-transmission. For brevity, defining $\mathbf{\Delta(t)} = \mathbf{H(t)} * \mathbf{X(t)} * \mathbf{H}^{\dagger}\mathbf{(-t)}$, Eq. (8) is rewritten as

$$\mathbf{y(t)} = [\mathbf{\Delta(t)}]_{\mathbf{N \times N}} * \mathbf{p(-t)} \quad (9)$$

Here $\mathbf{\Delta}$ is called generalized time-reversal operator since the element-by-element Fourier transform of $\mathbf{H(t)} * \mathbf{H}^{\dagger}\mathbf{(-t)}$, $\mathbf{H}(\omega)\mathbf{H}^{\dagger}(\omega)$, is usually called time-reversal operator [29]. Eq. (8) and Eq. (9) are sufficiently general for the purpose of this investigation.

[1]Some traditional receiver processing functions such as diagonalizing the matrix in Eq. (9) below are moved to the transmitter to simplify the receiver structure. Here the transmitter knows the channel and is able to optimize the transmission. These functions are implicitly absorbed in $\mathbf{X(t)}$ at this point.

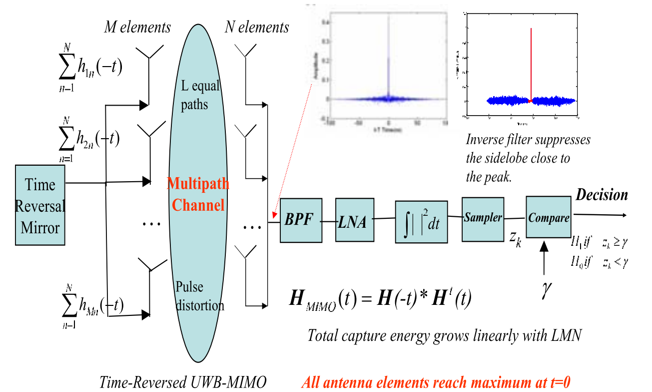

Fig. 1. The System Block Diagram of Time-Reversed Impulse MIMO.

To simplify receiver detection, a linear scheme is proposed here; the signal pulses received by the N antennas are pulse-shaped, linearly weighted, and linearly combined:

$$z(t) = \sum_{n=1}^{N} w_n(t) * y_n(t) = \mathbf{w(t)}^{\dagger} * \mathbf{y(t)} =$$

$$\mathbf{w(t)}^{\dagger} * \mathbf{H(t)} * \mathbf{X(t)} * \mathbf{H}^{\dagger}(-\mathbf{t}) * \mathbf{p}(-\mathbf{t}) \quad (10)$$

where $\mathbf{w} = [\mathbf{w_1(t)}, \mathbf{w_2(t)}, ..., \mathbf{w_N(t)}]^{\dagger}$. The right side of Eq. (10) is a scalar that also gives

$$z(t) = tr\left\{\mathbf{p}(-\mathbf{t}) * \mathbf{w}^{\dagger}(\mathbf{t}) * \left[\mathbf{H(t)} * \mathbf{X(t)} * \mathbf{H}^{\dagger}(-\mathbf{t})\right]_{\mathbf{N}\times\mathbf{N}}\right\} \quad (11)$$

where “tr” denotes the trace of an matrix. One goal of research is to make $z(t)$ resemble $\delta(t)$.

Let us make two observations about Eq. (8) and Eq. (9). If the operator $\mathbf{\Delta(t)}$ is diagonalized and the n-th diagonal element is $\Lambda_n(t)$, then Eq. (9) is simplified as

$$y_n(t) = \Lambda_n(t) * p_n(-t) \qquad n = 1, 2, ..., rank[\mathbf{\Delta(t)}] \quad (12)$$

In this special case, the whole system can be viewed as N independent channels. $\Lambda_n(t)$ is explained as the impulse response of the n-th effective channel. If these independent channels are used to carry the same symbols, the linear scheme as defined in Eq. (10) can be used to maximize the spatio-temporal diversity gain.

On the other hand, Eq. (12) can be used to maximize the capacity of the channel. The independent parallel channels in Eq. (12) can be used for different streams of symbols. In this case the elements of $\mathbf{X(t)}$ are used to represent parallel streams of symbols. If the N channels can carry identical symbol rates, the channel capacity of the MIMO is N times that of a single channel (SISO). Note the rank of the $\mathbf{\Delta(t)}$ is determined by the channel and numbers of transceiver antennas, and also satisfies $rank(\mathbf{\Delta(t)}) \leq \mathbf{min(M, N)}$. To simplify the following discussion, without loss of generality we assume $M \geq N$.

To gather insight, let us consider these two special applications: (1) the goal is to maximize the diversity gain; (2) the goal is to maximize the channel capacity.

B. Time-Reversed Impulse MIMO for Optimum Diversity

The objective here is to maximize the $z(t)$ in Eq. (11). Three limitations are of practical interest: (1) $p_n(t) = p(t)$, $n = 1, ..., N$ are identical for the n-th antenna; or $\mathbf{p}(-\mathbf{t}) = \alpha \mathbf{I_{N\times 1}} \mathbf{p}(-\mathbf{t})$. (2)$\mathbf{X(t)}$ is diagonal with its m-th diagonal element $x_{mm}(t) = \alpha \times p(t)$, implying that the M antennas send the same waveforms; Here α is information-bearing scalar during a symbol interval; or, $\mathbf{X(t)} = \alpha \mathbf{I_{M\times M}} \mathbf{p(t)}$ where $\mathbf{I_{M\times M}}$ is a $M \times M$ identity matrix with its diagonal elements being ones. (3) $\mathbf{w(t)} = \mathbf{I_{N\times 1}} \delta(\mathbf{t})$, implying $z(t) = \sum_{n=1}^{N} y_n(t)$.

The first two assumptions suggest using $q_m(t) = \sum_{n=1}^{N} h_{mn}(-t) * [p(-t) * p(t)]$ as the pre-filter for the m-th transmit antenna. For a chirp signal $p(t)$, $p(t) * p(-t) = \delta(t)$, so $q_m(t) = \sum_{n=1}^{N} h_{mn}(-t)$. Using a chirp signal we can pay our attention to the impulse nature of MIMO. Another choice is to choose very short pulses, say $p_n(t) \approx \delta(t)$ so the transmit array does not need to use pulse shaping at all. The two approaches are equivalent but the chirp one is believed to be more simple for implementation.

With the three simplifications, Eq. (11) is derived as

$$z(t) = tr[\mathbf{1_{N\times N}} \delta(\mathbf{t}) * \mathbf{H(t)} * \mathbf{H}^{\dagger}(-\mathbf{t})] * \alpha[\mathbf{p(t)} * \mathbf{p}(-\mathbf{t})] \quad (13)$$

where all the entries of $\mathbf{1_{N\times N}}$ are ones. The role of $\mathbf{1_{N\times N}}$ here is to sum up all the entries of the matrix $\mathbf{H(t)} * \mathbf{H}^{\dagger}(-\mathbf{t})$. Or, Eq. (13) is given by

$$z(t) = \alpha \Gamma(t) * [p(t) * p(-t)] \quad (14)$$

where we define

$$\Gamma(t) = tr(\mathbf{1_{N\times N}} \delta(\mathbf{t}) * \mathbf{H(t)} * \mathbf{H}^{\dagger}(-\mathbf{t})) \quad (15)$$

For a chirp pulse or Dirac pulse $p(t)$, Eq. (14) is reduced to $z(t) = \alpha \Gamma(t)$.

The elements of $\mathbf{H(t)} * \mathbf{H}^{\dagger}(-\mathbf{t})$ are expressed as

$$\left[\mathbf{H(t)} * \mathbf{H}^{\dagger}(-\mathbf{t})\right]_{nk} = \sum_{m=1}^{M} h_{nm}^{\dagger}(-t) * h_{km}(t) \quad n, k = 1, 2, ...N \quad (16)$$

The cross-correlations corresponds to terms of $n \neq k$, while the auto-correlations $n = k$. Eq. (15) is expanded in a term-by-term form to gather insight:

$$\Gamma(t) = \underbrace{\sum_{n=1}^{N} \left[\sum_{m=1}^{M} h_{nm}(-t) * h_{nm}(t)\right]}_{Coherent\ signal\ (Sharp\ Peak)} +$$

$$\underbrace{\sum_{n=1}^{N} \left\{ \left[\sum_{m=1, k\neq n}^{M} h_{nm}(-t)\right] * \left[\sum_{k=1, k\neq n}^{M} h_{km}(t)\right] \right\}}_{Incoherent\ signal} \quad (17)$$

The first part of Eq. (17) only involves all the auto-correlations, while the incoherent part all the cross-correlations. All the terms of $h_{mn}(-t) * h_{mn}(t)$ reaches their maximum at the same time ($t = 0$), and these peaks give the energies of each $h_{mn}(t)$. As a result, the coherent part will dominant the total signal at the receiver. A simple scheme such as energy-detection can be used to detect the information-bearing scalar α in Eq. (14).

Due to the coherent summing, both transmit and receive antennas contribute to the total captured energy. This is not true, however, for systems without using time-reversal. In [3], it is found that doubling the number of transmit antennas, M, does not change the SNR, while doubling the number of transmit antennas, N, does. The received signal amplitudes after the N matched filters add coherently whereas the corresponding noise components add incoherently. Doubling N yields a 3 dB gain in SNR. But with the diversity order of UWB channels being inherently very large, increasing diversity through adding more transmit antennas is only marginal. In the time-reversal scheme, the final summing up at the receiver can be effectively viewed as after the MN matched filters. Doubling M also causes the same performance as doubling N.

Physically, the coherent part can be viewed as the coherent spatio-temporal focusing of the N MISO arrays. The energy is spatio-temporally focused at the $n-$th antenna element located at $\mathbf{r} = \mathbf{r_n}$, $n = 1, 2, ..., N$. Each MISO [60] consists of M antenna elements located at $\mathbf{r} = \mathbf{r_m}$, $m = 1, 2, ..., M$. The MN elements serve as discrete sensors to sample the continuous spatio-temporal transient electromagnetic fields. The coherent contributions of these N MISO arrays are given by

$$\varphi(\mathbf{r_n}, \mathbf{t}) = \sum_{\mathbf{m=1}}^{\mathbf{M}} \mathbf{h_{nm}}(-\mathbf{t}) * \mathbf{h_{nm}}(\mathbf{t}), \quad \mathbf{r} = \mathbf{r_n}, \ \ \mathbf{n = 1, 2, ..., N} \tag{18}$$

Ideal spatio-temporal focusing implies that $\varphi_{\mathbf{r_n}}(t) = E_n \delta(\mathbf{r} - \mathbf{r_n})\delta(\mathbf{t})$ where E_n is the energy received by the n-th MISO array at $\mathbf{r} = \mathbf{r_n}$. If we superpose the N spatio-temporally focused contributions, they will be added up independently to yield

$$\Gamma(t) = \sum_{n=1}^{N} \varphi(\mathbf{r_n}, \mathbf{t}) = \left[\sum_{n=1}^{N} E_n \delta(\mathbf{r} - \mathbf{r_n}) \right] \delta(t). \tag{19}$$

In this ideal case, the incoherent signal part in Eq. (17) disappears. The total energy that is obtained by integration over the whole space and time is $\sum_{n=1}^{N} E_n$. As a consequence, the N discrete sensors capture all the energies, without overlapping other locations (interference to others). Seen from Eq. (19), all the terms $\varphi_{\mathbf{r_n}}(t)$ are synchronous at all times and reach their maximum at $t = 0$. As shown in Eq. (18), however, these terms are only synchronous at their maximum at $t = 0$; non-ideal spatial focusing leads to energies overlapping other undesired locations described by the incoherent part of Eq. (17). One goal of time-reversed impulse MIMO is to exploit the global synchronous property at $t = 0$. A superposition of the received signal at different antenna sensors across the space will stack up energies coherently.

In the following let us pay attention to mathematically understanding the coherent signal in Eq. (15) and Eq. (17). The squared Frobenius norm of $\mathbf{H}(\mathbf{t})$, $\mathbf{H_F^2}(\mathbf{t})$, is defined as

$$\mathbf{H_F^2}(\mathbf{t}) = \mathbf{tr}[\mathbf{H}(\mathbf{t}) * \mathbf{H}^\dagger(-\mathbf{t})] = \sum_{\mathbf{m=1}}^{\mathbf{M}} \sum_{\mathbf{n=1}}^{\mathbf{N}} \mathbf{h_{mn}}(\mathbf{t}) * \mathbf{h_{mn}}(-\mathbf{t}) \tag{20}$$

The first part of $\Gamma(t)$ in Eq. (17) is mathematically equal to $\mathbf{H_F^2}(\mathbf{t})$. Consider the MISO as a special case for $N = 1$. Eq. (20) simplifies as

$$\mathbf{H_F^2}(\mathbf{t}) = \mathbf{tr}[\mathbf{H}(\mathbf{t}) * \mathbf{H}^\dagger(-\mathbf{t})] = \sum_{\mathbf{m=1}}^{\mathbf{M}} \mathbf{h_m}(\mathbf{t}) * \mathbf{h_m}(-\mathbf{t}) \tag{21}$$

which is exactly the expression for MISO. The familiar definition of the Frobenius norm is given by [1]

$$\mathbf{H_F^2} = \mathbf{tr}[\mathbf{H}\mathbf{H}^\dagger] = \sum_{\mathbf{m=1}}^{\mathbf{M}} \sum_{\mathbf{n=1}}^{\mathbf{N}} |\mathbf{h_{mn}}|^{\mathbf{2}} \tag{22}$$

where h_{mn} are the channel gains. Due to the assumption of narrowband frequency flat fading, the convolution in the UWB MIMO degenerates to the simple product in Eq. (22). $\mathbf{H_F^2}(\mathbf{t})$ may be interpreted as the total energy of the channel and satisfies

$$\mathbf{H_F^2}(\mathbf{t}) = \sum_{\mathbf{n=1}}^{\mathbf{N}} \lambda_{\mathbf{n}}(\mathbf{t}) \tag{23}$$

where $\lambda_n(t)$ ($n = 1, 2, ..., N$) are the eigenvalues of $\mathbf{H}(\mathbf{t}) * \mathbf{H}^\dagger(-\mathbf{t})$.

C. Time-Reversed Impulse MIMO for Optimum Capacity

The starting point of this application is Eq. (12) that is copied here for convenience

$$y_n(t) = \Lambda_n(t) * p_n(-t) \qquad n = 1, 2, ..., rank[\mathbf{\Delta}(\mathbf{t})] \tag{24}$$

where the coupled operator $\mathbf{\Delta}(\mathbf{t})$ is diagonalized with its n-th diagonal elements being $\Lambda_n(t)$. As mentioned previously, $rank[\mathbf{\Delta}(\mathbf{t})]$ is bounded by N if $M \geq N$. Without loss of generality, $p_n(-t)$ are assumed to have unit energies. Let us also assume that the information symbols a_n, $n = 1, 2, ..., N$, are modulated in such a way that

$$\Lambda_n(t) = a_n \ E_n \ s_n(t) \quad n = 1, 2, ..., N \tag{25}$$

where for the n-th symbol $s_n(t)$ is a pulse wave shape of finite duration and bandwidth B_n. We constrain the normalized transmit symbol energy of each antenna element such that $E_n \leq 1$, $n = 1, 2, ..., N$. Then, after adding an zero-mean additive white Gaussian noise (AWGN) process $n_n(t)$ of power spectral density σ_n^2 at the n-th receive antenna element, Eq. (24) can be rewritten as

$$y_n(t) = E_n \ \chi_n(t) + n_n(t) \qquad n = 1, 2, ..., N \tag{26}$$

where $\chi_n(t) = a_n s_n(t) * p_n(-t)$ with bandwidth B_n and signal energy $E_{s\Lambda_n}$ within a symbol duration T_s, and $n_n(t)$'s are statistically independent. Eq. (26) can be viewed as N

independent, parallel channels. The SNR for the n-th independent channel is expressed in terms of the signal energy per symbol $\rho_n E_n$ where $\rho_n = E_{s\Lambda_n}/\sigma_n^2 B_n T_s$. For a given $\mathbf{H}(\mathbf{t})$, the capacity of the n-th channel is

$$I_n = B_n \; log_2(1 + \rho_n E_n) \quad n = 1, 2, ..., N \tag{27}$$

Since the channels are independent, $E_n = 1$, $n = 1, 2, ..., N$ maximizes the capacity in each channel [4]. The average channel capacity per channel is given by [4]

$$I_s/N = \frac{1}{N}\sum_{n=1}^{N} B_n \; log_2(1 + \rho_n) \tag{28}$$

Eq. (28) upper bounds the average capacity per antenna element.

D. Future Work

In the theoretical aspects, we will take advantage of spatio-temporal focusing, a new physical phenomenon governed by transient electromagnetics, which is unique to time-reversed impulse systems. We are particularly interested in extending the current work to the framework of MIMO to improve the spatio-temporal focusing.

The similarity of the UWB communications to that of underwater acoustic (UWA) communications motivates a unified view of the two systems. Common issues include rich multipath and fading. Equalization to compensate for inter-symbol-interference (ISI) is critical. Time-reversal is promising for both. Frequency-shift-keying (FSK) is the primary practical scheme that works for UWA. Phase-shift-keryng (PSK) is promising for high-data rates, but suffers from random phase noise caused by the ocean [35]. One wonder if the concept of "impulse radio" can be applied to UWA communications. Modulation schemes based on carrierless pulses such as pulse position modulation (PPM) have some advantages, especially for high-frequency UWA communications in the bandwidth of e.g. 25-50 kHz. The relative bandwidth of this system satisfies the definition of UWB, according to FCC. This large bandwidth justifies the use of UWB wireless technologies to UWA communications.

III. Summary

A theory of time-reversed impulse MIMO is given for UWB communications. One goal of the proposed research is to investigate time-reversal based non-coherent reception as an alternative to coherent communications. The approach takes advantage of the unique characteristics of impulse radio, through a new paradigm of using time-reversal combined with MIMO. In this paradigm, only a noncoherent energy detector is required in the receiver that will be cost-effective.

Acknowledgment

The author thanks Drs. Brian Sadler and Robert Ulman for initial support for this work. He also thanks Drs. Santanu K. Das, T. C. Yang, and W. B. Wang for useful discussions. His graduate C. M. Zhou helps to verify some derivations.

This work is funded in part by the Army Research Laboratory and the Army Research Office through a STIR grant (W911NF-05-1-0468) and a DURIP grant (W911NF-05-1-0111). The author is sponsored by ONR Summer Faculty program through the American Society for Engineering Education (ASEE) to work at Naval Research Laboratory in the summer of 2006.

References

[1] Paulraj, R. Nabar, and D. Gore, *Introduction to Space-Time Wireless Communications*, Cambridge University Press, 2003.

[2] H. L. Van Trees, *Optimum Array Processing*, John Wiley and Sons, 2002.

[3] M. Weisenhorn and W. Hirt, "Performance of Binary Andipodal Signaling over the Indoor UWB MIMO," *IEEE ICC'03*, pp. 2872-78, May 2003.

[4] J. H. Winters, "On the Capacity of Radio Communication Systems with Diversity in a Rayleigh Fading Environment," *IEEE J. Select. Area Commun. (JSAC)*, Vol. 5, No. 5, pp. 871-878, June 1987.

[5] G. J. Foschini, "Layered Space-Time Architecture for Wireless Communication in Fading Environment," *Bell System Tech. J.*, pp. 41-59, Autumn 1996.

[6] G. J. Foschini and M. Gans, "On Limits of Wireless Communications in a Fading Environment When Using Multiple Antennas," *Wireless Personal Commun.*, pp. 311-35, March 1998.

[7] M.Z. Win and R.A. Scholtz, "Impulse radio: How it works" *IEEE Commun. Lett.*, vol.2, no.2, pp.36-38, Feb. 1998.

[8] M. Z. Win and R. A. Scholtz, "Ultra-wide bandwidth time-hopping spread-spectrum impulse radio for wireless multiple-access communications," *IEEE Trans. Commun.*, vol.48, no. 4, pp.679-691, April 2000.

[9] M. Z. Win and R. A. Scholtz, "On the robustness of ultra-wide bandwidth signals in dense multipath environments," *IEEE Commun. Lett.*, vol. 2, no. 2, pp. 51-53, Feb. 1998.

[10] M. Z. Win and R. A. Scholtz, "On the energy capture of ultra-wide bandwidth signals in dense multipath environments," *IEEE Commun. Lett.*, vol. 2, no. 9, pp. 245-247, Sept. 1998.

[11] R. J. Cramer, R. A. Scholtz, and M. Z. Win, "An Evaluation of the Ultra-Wideband Propagation Channel," *IEEE Trans. Antennas Propagat.*, vol. 50, no. 5, pp. 561-570, May 2002.

[12] D. Cassioli, M. Z. Win and A. F. Molisch, "The Ultra-Wide Bandwidth Indoor Channel: from Statistical Model to Simulations," *IEEE J. Select. Areas Commun.*, vol. 20, no. 6, pp. 1247-1257, Aug. 2002.

[13] M. Z. Win and R. A. Scholtz, "Characterization of ultra-wide bandwidth wireless indoor communications channel: A communication theoretic view," *IEEE J. Select. Areas Commun.*, vol. 20, no. 9, pp. 1613-1627, Dec. 2002.

[14] A. Giorgetti, M. Chiani, and M. Z. Win, "The effect of narrowband interference on wideband wireless communication systems," *IEEE Trans. Commun.*, vol. 53, no. 12, pp. 2139-2149, Dec. 2005.

[15] M.Z. Win, "A unified spectral analysis of generalized time-hopping spread-spectrum signals in the presence of timing jitter," *IEEE J. Select. Areas Commun.*, vol.20, no.9, pp.1664-1676, Dec. 2002.

[16] A. Ridolfi and M. Z. Win, "Ultrawide bandwidth signals as shot-noise: a unifying approach," *IEEE J. Select. Areas Commun.*, vol. 24, no. 4, pp. 899-905, Apr. 2006.

[17] T. Q. S. Quek and M. Z. Win, "Analysis of UWB transmitted reference communication systems in dense multipath channels," *IEEE J. Select. Areas Commun.*, vol. 23, no. 9, pp. 1863-1874, Sept. 2005.

[18] W. Suwansantisuk, M. Z. Win, and L. A. Shepp, "On the performance of wide-bandwidth signal acquisition in dense multipath channels," *IEEE Trans. Veh. Technol.*, vol. 54, no. 5, pp. 1584-1594, Sept. 2005.

[19] W. Suwansantisuk and Moe Z. Win, "Multipath aided rapid acquisition: Optimal search strategies," *IEEE Trans. Inform. Theory*, vol. 52, 2006, to be published.

[20] R.C. Qiu, H.P. Liu, X. Shen, and M. Guizani, "Ultra-wideband for Multiple Access," *IEEE Commun. Mag.*, vol.43, pp. 80-87, Feb. 2005.

[21] R. C. Qiu, R. Scholtz, and X. Shen, "Ultra-Wideband Wireless Communications– A New Horizon," Editorial on Special Session on UWB, *IEEE Trans. Veh. Technol.*, Vol. 54, No. 5, Sept. 2005.

[22] R. C. Qiu, H. Liu, and X. Shen, "Ultra-Wideband for Multiple Access," *IEEE Commun. Mag.*, Vol. 43, No. 2, pp. 80-87, Feb. 2005.

[23] X. Shen, M. Guizani, H. H. Chen, R. Qiu, A. F. Molisch, "Ultra-wideband Wireless Communications," Editorial on Special Issue on UWB, *IEEE J. Select. Areas Commun.,*Vol. 24, 2nd Quarter 2006.

[24] R. C. Qiu, X. Shen, M. Guizani and T. Le-Ngoc, "Introduction," Book Chapter, *UWB Wireless Communications*, Editors: X. Shen, M. Guizani, R. C. Qiu, T. Le-Ngoc, John Wiley, 2006.

[25] A. Derode, P. Roux, and M. Fink, "Robust Acoustic Time Reversal with High-order Multiple Scattering," *Phys. Rev. Letters*, Vol. 75, pp. 4206–4209, 1995.

[26] M. Fink, "Time Reversed Acoustics," *Physics Today*, pp. 34–40, 1997.

[27] M. Fink, "Time-reversed Acoustics," *Scientific American*, pp. 91–97, 1999.

[28] D. Rouseff, D. R. Jackson, W. L. J. Fox, C. D. Jones, J. A. Ritcey and D. R. Dowling, "Underwater Acoustic Communication by Passive-Phase Conjugation: Theory and Experimental Results," *IEEE J. Ocean. Eng.*, Vol. 26, pp. 821-831, 2001.

[29] M. Tanter, J. F. Aubry, J. Gerber, J. L. Thomas, and M. Fink,"Optimal Focusing by Spatio-temporal Inverse Filter," *J. Acoust. Soc. Am.*, Vol. 110, No. 1, pp. 37-47, July 2001.

[30] G. Montaldo, M. Tanter, and M. Fink,"Real Time Inverse Filter Focusing through Iterative Time Reversal," *J. Acoust. Soc. Am.*, Vol. 115, No. 2, pp. 768-775, Feb. 2004.

[31] D. R. Jackson and D. R. Dowling, "Phase Conjugation in Underwater Acoustics," *J. Acoust. Soc. Am.*, Vol. 89, pp. 171–181, 1990.

[32] D. R. Dowling and D. R. Jackson, "Narrow-band Performance of Phase Conjugate Arrays in Dynamic Random Media," *J. Acoust. Soc. Am.*, Vol. 91, pp. 3257–3277, 1992.

[33] D. R. Dowling, "Acoustic Pulse Compression Using Passive Phase Conjugate Processing," *J. Acoust. Soc. Am.*, Vol. 95, pp. 1450–1458, 1994.

[34] W. A. Kuperman, W. S. Hodgkiss, H. C. Song, T. Akal, C. Ferla, and D. R. Jackson, "Phase Conjugation in the Ocean: experimental demonstration of an acoustic time-reversal mirror," *J. Acoust. Soc. Am.*, Vol. 103, No. 1, pp. 25–40, 1998.

[35] T. C. Yang, "Temporal Resolution Of Time-Reversal and Passive-Phase Conjugation For Underwater Acoustic Communications," *IEEE J. Oceanic Eng.*, Vol. 28, pp. 229–245, 2003.

[36] K. B. Smith, A. M. Abrantes and A. Larraza, "Examination of Time Reversal Acoustics in Shallow Water and Applications to Noncoherent Underwater Communications," *J. Acoust. Soc. Am.*, Vol. 113, No. 6, pp. 3095–3110, 2003.

[37] M. Heinemann, A. Larraza and K. M. Smith, "Experimental Studies of Applications of Time Reversal Acoustics to Noncoherent Underwater Communications," *J. Acoust. Soc. Am.*, Vol. 113, No. 6, pp. 3111–3116, 2003.

[38] A. Derode, A. Toupin, J. de Rosny, M. Tanter, S. Yon and M. Fink, "Taking advantage of Multiple Scattering to Communicate with Time-Reversal Antennas," *Phys. Rev. Letters*, Vol. 90, 2003.

[39] L. G. Van Atta, "Electromagnetic Reflector," U. S. Patent 2 908 002, Oct. 6, 1959.

[40] G. Lerosey, J. de Rosny, A. Tourin, A. Derode, G. Montaldo, and M. Fink, "Time Reversal of Electromanetic Waves," *Phy. Rev. Lett.*, Vol. 92, No. 19, 193904, 2004.

[41] B. E. Henty and D. D. Stancil, "Multipath-Enabled Super-Resolution for rf and Microwave Communication using Phase-Conjugate Arrays," *Phy. Rev. Lett.*, Vol. 93, 243904, 2004.

[42] T. Strohmer, M. Emami, J. Hansen, G. Papanicolaou and A. Paulraj, "Application of Time-reversal with MMSE Equalizer to UWB Communications," *Proceedings of Globecom Conference,* Dallas, Texas, pp. 3123-3127, Dec. 2004.

[43] P. Kyritsi, G. Papanicolaou, P. Eggers and A. Oprea, "MISO Time Reversal and Delay-spread Compression for FWA Channels at 5 GHz," *IEEE Antennas and Wireless Propagat. Lett.*, Vol. 3, No. 6, pp. 96-99, 2004.

[44] C. Oestges, A.D. Kim, G. Papanicolaeou, A.J. Paulraj, "Characterization of Space-time Focusing in Time-reversed Random Fields," *IEEE Trans. Antennas and Propagat.*, Vol. 53, No. 1, pp. 283-293, Jan. 2005.

[45] S. M. Emami, J. Hansen, A. D. Kim, G. Papanicolaeou, A. J. Paulraj, D. Cheung, C. Prettie, "Predicted Time Reversal Performance in Wireless Communications Using Channel Measurements," *IEEE Comm. Letters, to appear*.

[46] M. Emami, M. Vu, J. Hansen, G. Papanicolaou, and A. Paulraj, "Matched Filtering with Rate Back-off for Low Complexity Communications in Very Large Delay Spread Channels," *Proceedings of the Asilomar Conference 2004*, pp. 218-222, 2004.

[47] J. Hansen and A. Paulraj, "Design Approach for a Time Reversal Test Bed for Radio Channels," *Proceedings of the Eusipco 2004*, Vienna, Special Session on MIMO Prototyping, Sept. 2004.

[48] P. Kyritis and F. Lee, "Notes from AIM Workshop on Time Reversal Communications in Richly Scattering Environments," Oct. 18-22, 2004, available at http://www.aimath.org/WW N/timerev/timerev.pdf.

[49] H. T. Nguyen, J. B. Andersen and G. F. Pedersen, "The Potential Use of Time Reversal Techniques in Multiple Element Antenna Systems," *IEEE Communications Letters*, Vol 9, No. 1, pp. 40- 42, 2005.

[50] H. T. Nguyen, I. Z. Kovacs ,and P. Eggers, "Time Reversal Transmission Potential for Multi-user UWB Communications," *Wireless Personal Communications Conference,* Aalborg, Denmark, September 2005,

[51] G. Cepni, D. D. Stancil, Y. Jiang, and J. Zhu, "Microwave Signal Nulling Using Multiple Antennas and Time Reversal Method," *IEEE Vehicular Technol. Conf. (VTC'05*), Sweden, 2005.

[52] J. M. Moura, Y. Jin, D. D. Stancil, J. Zhu, A. Cepni, Y. Jiang, and B. Henty, "Single Antenna Time Reversal Adaptive Interference Cancellation," *IEEE ICASSP 2005,* pp. 1121-1124, 2005.

[53] S. Kaza, "Performance Analysis of Ultra-Wideband Transmitted Reference System and Enhancement Techniques," Department of Electrical and Computer Engineering, Master Thesis, Tennessee Technological University, Cookeville, TN, 2004.

[54] E. Akogun, R. C. Qiu and N. Guo, "Demonstrating Time Reversal in Ultra-wideband Communications Using Time Domain Measurements," *51st International Instrumentation Symposium*, 8-12 May 2005, Knoxville, Tennessee.

[55] E. Akogun, "Theory and Application of Time Reversal Technique to Ultra-Wideband Wireless Communications," Department of Electrical and Computer Engineering, Master Thesis, Tennessee Technological University, Cookeville, TN, 2005.

[56] N. Guo, R. C. Qiu, and B. M. Sadler, "An Ultra-Wideband Autocorrelation Demodulation Scheme with Low-Complexity Time Reversal Enhancement," *IEEE MILCOM'05*, Atlantic City, NJ, Oct. 17-20.

[57] R. C. Qiu, C. Zhou, N. Guo, and J. Q. Zhang, "Time Reversal with MISO for Ultra-Wideband Communications: Experimental Results, " Invited Paper**,** *IEEE Radio and Wireless Symposium*, San Diego, CA, Jan. 2006.

[58] C. Zhou and R. C. Qiu, "Spatial Focusing of Time-Reversed UWB Electromagnetic Waves in a Hallway Environment," *IEEE 38th Southeastern Symposium on System Theory (SSST 2006)*, March 5-7, 2006, Cookeville, TN, USA.

[59] N. Guo, R. C. Qiu, and B. M. Sadler, "A Transmitted Reference UWB System with Time Reversal Based on Experimental UWB Channel Measurements"*IEEE Trans. Wireless Comm.*, Submitted for publication, May 2006.

[60] R. C. Qiu, C. Zhou, N. Guo, J. Q. Zhang, "Time Reversal with MISO for Ultra-Wideband Communications: Experimental Results", *IEEE Antenna and Wireless Propagation Letters*, April 2006.

[61] R. C. Qiu. J. Q. Zhang, N. Guo, "Detection of Physics-Based Ultra-Wideband Signals Using Generalized RAKE and Multi-User Detection (MUD)," *IEEE J. Selected Areas in Commun. (JSAC),* the Second JSAC special issue on UWB Radio, Vol. 24, No. 2, May 2006.

[62] R. C. Qiu, Chapter "UWB Pulse Propagation Processes," *UWB Wireless Communications - A Comprehensive Overview*, Eurasip, 2005.

[63] R. C. Qiu, C. Zhou and Q. Liu, "Physics-Based Pulse Distortion for Ultra-Wideband Signals", *IEEE Trans. Veh. Tech.*, Vol. 54, No. 5, Sept. 2005.

[64] N. Guo and R. C. Qiu, "Improved Autocorrelation Demodulation Receivers Based on Multiple-symbol Detection for UWB Communications", *IEEE Trans. Wireless Communications,* to appear, 2006.

[65] R. C. Qiu, "A Generalized Time Domain Multipath Channel and Its Application in Ultra-Wideband (UWB) Wireless Optimal Receiver Design: Part III System Performance Analysis," *IEEE Trans. Wireless Communications,* to appear, 2006.

[66] R. C. Qiu, "A Generalized Time Domain Multipath Channel and its Application in Ultra-Wideband (UWB) Wireless Optimal Receiver Design: Part II Wave-Based System Analysis," *IEEE Trans. Wireless Communications,* Vol. 3, No. 11, pp. 2312-2324, Nov. 2004.

[67] R.C. Qiu, "A Study of the Ultra-wideband Wireless Propagation Channel and Optimum UWB Receiver Design (Part I)," *IEEE J. Selected Areas in Commun. (JSAC),* the First JASC special issue on UWB Radio, Vol. 20, No. 9, pp. 1628-1637, December 2002.